The Geometry of *N*-Hydroxymethyl Compounds. Part 5.[1] Studies on Ground-State Geometry and Reactions of *N*-(Hydroxymethyl)pentamethylmelamine and Related Compounds using MNDO Calculations

Richard J. Simmonds and Geeta Dua
Institute of Biological Sciences, University of Wales, Aberystwyth, UK SY23 3DD

MNDO and PM3 calculations of the most favoured conformations of antitumour *N*-hydroxymethylmelamines including *N*-(hydroxymethyl)pentamethylmelamine (**2**) and trimelamol indicate that the O–H group is orientated towards the closest ring nitrogen but is too distant for hydrogen bonding. Modelling of decomposition pathways of **2** using MNDO predicts that concerted loss of formaldehyde is not favoured. Loss of $[H_2COH]^+$ from oxygen-protonated **2** is also a high energy process, but loss of formaldehyde from deprotonated **2** is exothermic with a low activation barrier; this is the most likely decomposition mechanism under basic or neutral conditions. Under acidic conditions loss of water from protonated **2** to give an iminium ion is exothermic from *O*-protonated **2**, but the initial *O*-protonation is disfavoured over protonation on nitrogen, particularly ring nitrogens. Reaction of **2** with nucleophiles is difficult by S_N2 routes but proceeds exothermically with low activation energies by the S_N1 mechanism from protonated **2** to give products of similar thermodynamic stability to ring-protonated **2**. Reaction of *O*-protonated **2** with amines gives aminals that may decompose with low activation energies to pentamethylmelamine and a methylene iminium ion.

Hexamethylmelamine [**1**, HMM, 2,4,6-tris-(dimethylamino)-1,3,5-triazine] is an antitumour drug with activity against certain solid human tumours including ovarian carcinoma and small cell carcinoma of the lung.[2] Its mechanism of action is not known but it is inactive *in vitro* and is rendered active[3] by metabolic oxidative demethylation (Scheme 1). The first metabolic product is HMPMM (**2**), which is active *in vitro*. HMPMM decomposes in aqueous solution to give formaldehyde and pentamethylmelamine (PMM, **3**) but there is evidence[4] that formaldehyde toxicity is not the main cause of cytotoxicity to cancer cells. PMM undergoes further oxidative demethylation *in vivo* to give other hydroxymethyl derivatives with a lower antitumour activity than HMPMM. No cross-linking of DNA has been found from HMM and it is active against tumours that have become resistant to alkylating agents; these observations imply that it should not be classified as an alkylating agent in its mode of antitumour action. On the other hand, the triazine portion of HMM may become attached[5] to DNA when HMM is metabolised by hepatic microsomal preparations and HMPMM does react with certain nucleophiles including biological macromolecules[5] and glutathione[6] *in vitro*, so the cytotoxicity of melamines may arise from reaction with nucleophilic biomolecules.

HMM has low water-solubility that causes problems in its medicinal use and much work on improving HMM as an anticancer drug has concentrated on water-soluble analogues. A water-soluble analogue of HMM, which has shown promise in clinical trials,[4] is trimelamol. The discovery that oxidative demethylation of melamines is much slower in humans than rodents stimulated interest in this compound as an antitumour drug since it makes sense to concentrate on hydroxymethylmelamines, such as trimelamol, which have intrinsic activity rather than expect them to be formed *in vivo* by metabolism of methylamino precursors. A difficulty with trimelamol is its plasma half-life[7] which is only six minutes in humans and so longer lived analogues are currently sought.

The rate of decomposition of hydroxymethyltriazines to liberate formaldehyde in aqueous solutions depends on many

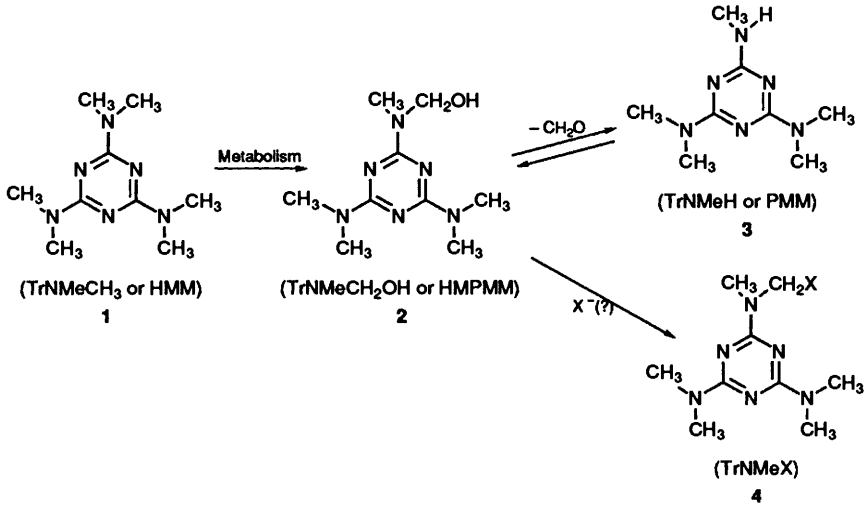

Scheme 1

factors[7] including pH and the presence of other dissolved species. Although such reactions are clearly of importance in the elucidation of mechanisms of action of these compounds and in the design of analogues, the decomposition mechanism remains unknown. Given that either protonation or deprotonation are reasonable first steps, anionic, cationic and concerted mechanisms as shown in Schemes 2–4 (R′ = Tr) may be proposed. The decomposition mechanisms of some other hydroxymethylamines are better known. Bundgaard[8] studied the rates of decomposition of *N*-(hydroxymethyl)amides under physiological conditions to produce formaldehyde and amides and concluded that the decomposition occurs (Scheme 2, R′ = RCO) through an anionic intermediate undergoing rate determining N–CH_2OH bond cleavage.

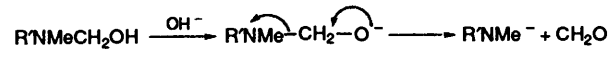

Scheme 2 Anionic mechanism for the decomposition of *N*-hydroxymethyl compounds

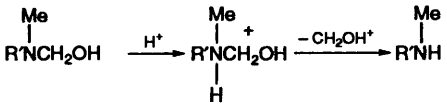

Scheme 3 Cationic mechanism for the decomposition of *N*-hydroxymethyl compounds

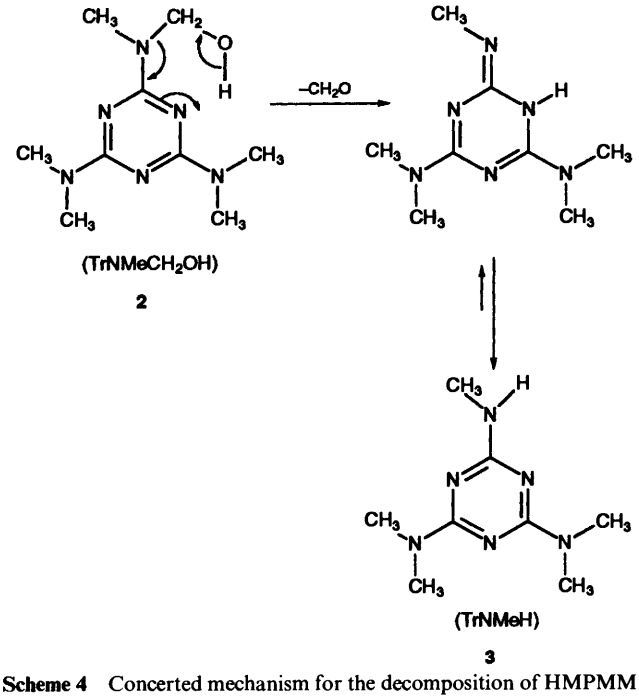

Scheme 4 Concerted mechanism for the decomposition of HMPMM

Hydroxymethylamines are important intermediates—for example in the industrial preparation of melamine–formaldehyde resins—and extensive kinetic studies[9] have been published on the mechanisms of the polymerization reaction. These reveal a highly complex system which may be acid or base catalysed. Other reactions with nucleophiles have been little studied but the polymerization work suggests that the system is complex and the experimental approach would yield information very slowly. Studies[10] on *N*-(hydroxymethyl)-amides are more wide-ranging but less detailed and it is believed that they usually react with carbon nucleophiles by an acid-catalysed mechanism (Scheme 5, R′ = RCO) although base-catalysis is also known.

Our studies on the mechanisms of decomposition of hydroxymethyl compounds have made use of molecular orbital calculations to establish correlations between ground state

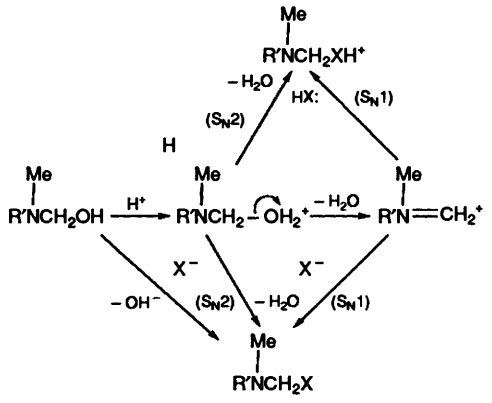

Scheme 5 Mechanisms considered for nucleophilic substitution reactions of *N*-hydroxymethyl compounds

structures and decomposition rates and to examine the energies of competing reaction pathways. We have established[11] that MNDO calculations predict realistic geometries for *N*-hydroxymethyl derivatives and that the calculated N–CH_2OH bond lengths of *N*-(hydroxymethyl)amides correlate well with their physiological half-lives. With *N*-(hydroxymethyl)triazenes we established[1] experimentally that their half-lives are too short for intrinsic antitumour activity and showed by calculation that a base-catalysed decomposition was favoured over acid-catalysed or concerted routes. On the other hand Iley *et al.*[12] obtained evidence that hydroxymethylpyridyltriazenes decompose through a cyclic six-membered transition state in which an amino or hydroxylic nucleophile acts as both proton acceptor and proton donor.

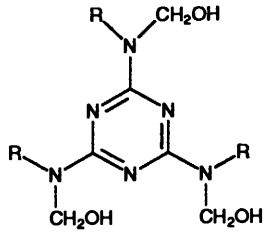

With the aim of gaining insight into the mechanism(s) of reaction, decomposition and antitumour action of *N*-(hydroxymethyl)melamines we have used MNDO calculations to find their ground state structures, possible decomposition pathways, and their reaction pathways with simple nucleophiles such as MeOH, NH_3 and H_2S. Also we have been seeking relationships that will be of help in the design of more stable analogues of the hydroxymethylmelamines or for the selection of synthetic routes to analogues of HMPMM.

Results and Discussion

Our initial work used partial optimizations and an early version of MOPAC[13] and so stationary states identified were reexamined using the latest implementation. The use of MOPAC 93[14] to reoptimize triazine structures previously fully optimized using MOPAC version 2 usually reduced the enthalpy a little (*e.g.* by 8 kJ mol^{-1} for HMPMM) without significant conformational change. An exception was TrNMeCH_2S^- which increased in enthalpy by 59 kJ mol^{-1} again without significant conformational change. All the (non-triazine) small molecules shown in Table 2 (see later) were recalculated and found to have ground state structures and energies as reported in the most recent literature[15] except

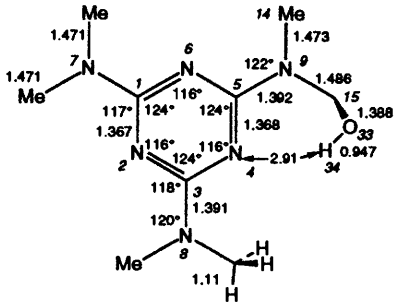

Fig. 1 Optimized structure of HMPMM (**2**) showing the numbering system (in italics), bond angles and bond lengths

Table 1 Half-life of tris(hydroxymethyl)melamine derivatives (**5**) in water at 37 °C and pH 7.5 compared with MNDO calculated bond lengths and net atomic charges

			Charge	
R	$t_{\frac{1}{2}}$/min	N–CH_2/Å	N(9)	C(15)
Me	120	1.4863	−0.4074	0.3390
CH_2CN	275	1.493	−0.3908	0.3433
$CH_2C{\equiv}CH$	450	1.487	−0.3969	0.3447
CH_2CF_3	690	1.498	−0.3950	0.3515

H_3O^+ which gave a slightly higher enthalpy and formaldehyde (slightly lower). Fully optimizing structures, previously optimized with the triazine ring fixed as described in the experimental section, decreased the enthalpy, typically by 1–10 kJ mol^{-1}, but up to 40 kJ mol^{-1} for S-containing and ring-protonated compounds. The values given below are calculated using MNDO with full optimization by the default methods in MOPAC 93 unless otherwise stated except for the reaction paths which normally relate to structures partially optimized using MOPAC version 2. The fully optimized stationary states given in Tables 2 and 3 are thus lower in enthalpy than the partially optimized stationary states that are normally displayed in Figs. 2–4.

Ground State Structures.—A full optimization of the geometry of HMPMM gave the structure shown in Fig. 1; the numbering of atoms is that used in our calculations and for specifying atoms in this paper, but it is not consistent with IUPAC nomenclature. The CH_2OH is positioned so that the H is directed towards the nearest ring nitrogen (N-4) but the O is out of the ring plane resulting in an OH ··· N(4) distance of 2.92 Å, which is too long for hydrogen-bonding. No lower enthalpy conformation could be found by making the NCH_2OH coplanar with the ring to permit strong hydrogen-bonding and reoptimizing the structure. Since MNDO is considered poor at modelling hydrogen bonds, the geometry was also studied using PM3 which gave a gound state at −78 kJ mol^{-1} with a similar structure to that obtained using MNDO—the planar hydrogen-bonded geometry was unstable relative to one in which the O is out-of-plane with the H of OH pointing towards N(4) but 2.67 Å from it. Evidently the electron-deficiency of the triazine results in the ring nitrogens having little ability to accept hydrogen bonds. Both the MNDO and PM3 optimized geometries were similar to the crystal structure which shows[16] no intramolecular hydrogen-bonding (OH ··· N = 2.99 Å) and an out-of-plane oxygen atom.

In MNDO-calculated ground states of *N*-hydroxymethylamides, N–CH_2OH bond lengths and charges on the N of the *N*-hydroxymethyl group have proved[11] reliable indicators of the stabilities of these compounds and so we sought similar relationships amongst trimelamol analogues whose half lives have recently been reported.[7] Trimelamol (**5**, R = Me) has a similar optimum geometry [OH ··· N(4) = 2.93 (MNDO), 2.98 Å (PM3)] to that of HMPMM and this was compared with the geometries of three other trimelamol derivatives. Unlike the hydroxymethylamides the calculated N–CH_2OH bond lengths and net atomic charges on N in the optimum structures do not show any relationship to the physiological half-lives (Table 1), but the net atomic charge on C in NCH_2OH does correlate (r^2 = 0.96); more positive charge on C parallels increased stability of trimelamol derivatives. This could be taken as evidence that the mechanism of decomposition is different from that of the hydroxymethylamides although another difference is that, instead of being reasonably constant, these parameters vary with conformation. For example, rotation of the CH_2–OH bond in HMPMM from its optimum position (with shortest OH ··· N-4 distance and an N–CH_2–O–H dihedral of 79°) caused the N–CH_2OH bond to shorten by up to 0.02 Å (when the NCH_2–OH dihedral angle was 180°) and the net atomic charge on nitrogen to change from −0.409 (NCH_2–OH dihedral 79°) to −0.364 (at 180°) and then back to −0.423 units (at 320°).

Ground-state structures of compounds expected to result from reaction of HMPMM with simple nucleophiles were studied. In each case the dimethylamino groups attached directly to the ring were approximately coplanar with the ring, thus allowing maximum conjugation of the nitrogen lone pair with the triazine. Those structures in which the OH in HMPMM is replaced with SH or NH_2 have similar structures to HMPMM itself, with a hydrogen from SH or NH_2 directed towards N(4) but too distant for hydrogen bonding (3.1 and 3.0 Å, respectively). Closing the distance between this hydrogen and N-4 raises the enthalpy. When CH_2NMe_2 replaces the CH_2OH the CH_2 remains approximately coplanar with the ring but the NMe_2 rotates to be nearly at right angles to the plane. When CH_2OMe or CH_2NHMe is attached to N-9 the CH_2 is orientated virtually at right angles to the ring and the Me group is directed away from the ring; the NH ··· N(4) distance is still only 3.1 Å in the methylamino compound, however. Enthalpies for ground state structures are given in Table 2; in this table and the remainder of the paper the 4,6-bis-(dimethylamino)-1,3,5-triazine group is denoted by Tr so the chemical structure of HMPMM is abbreviated to $TrNMeCH_2OH$.

Optimum structures arising from protonation of HMPMM at any of the nitrogens or on the oxygen were calculated. Protonation at N-4 allows close interaction with the oxygen and this is the energetically most favoured protonation position. The optimum structure is similar to HMPMM with the oxygen directed towards the additional proton but separated from it by 2.77 Å; the proton covalently bound to oxygen points away from the ring. Thermodynamically the susceptibility towards protonation is ring-N > exocyclic-N > O but the difference between the most and least stable protonated species is less than 100 kJ mol^{-1} and so reactions through any of these may be reasonably considered. Protonation of HMPMM by H_3O^+ on oxygen liberates 86 kJ mol^{-1} and deprotonation of the OH in HMPMM by OH^- is also exothermic (ΔH = −240 kJ mol^{-1}) and so reactions of these ionized forms are feasible under physiological conditions.

Protonation of HMPMM and analogues of general structure $TrNMeCH_2X$ (X = OMe, NH_2, NHMe, NMe_2, SH) is accompanied by some systematic changes. Protonation on the O, N or S in X lengthens the C–X bond considerably and gives a minimum enthalpy conformation with the proton directed towards N-4 but too distant for strong hydrogen-bonding. Also the bond orders between C(5)–N(9) and C–X are reduced while that at N(9)–CH_2 is increased. In short, the X-protonated structure distorts to resemble an iminium ion associated with XH. Protonation on N-9 is accompanied by lengthening of the

Table 2 Enthalpies of formation ($\Delta_f H$) of fully optimized ground state structures calculated using MNDO

Neutral Compound	$\Delta_f H$/kJ mol^{-1}
$TrNMeCH_2OH$	−36
$TrNMeCH_2NH_2$	186
$TrNMeCH_2NMe_2$	215
$TrNMeCH_2NHMe$	190
$TrNMeCH_2SH$	191
$TrNMeCH_2OMe$	4
TrNMeH	146
H(N4)TrNMe	217
H_2O	−255
CH_2O	−138
CH_3OH	−240
NH_3	−27
H_2S	16
$HNMe_2$	−28
H_2NMe	−32
Anion	
OH^-	−24
CH_3O^-	−166
$TrNMe^-$	−48
$TrNMeCH_2O^-$	−45
$TrNMeCH_2S^-$	126
Cation	
$H(N4)TrNHMe^+$	771
$TrNMeCH_2O(Me)H^+$	730
$H(N4)TrNMeCH_2OMe^+$	615
$TrNMeHCH_2OMe^+$	699
$TrNMeCH_2OH_2^+$	700
$H(N2)TrNMeCH_2OH^+$	598
$H(N4)TrNMeCH_2OH^+$	589
$H(N6)TrNMeCH_2OH^+$	594
$H(N7)TrNMeCH_2OH^+$	670
$H(N8)TrNMeCH_2OH^+$	675
$TrNMeHCH_2OH^+$	671
$TrNMeCH_2^+$	932
$TrNMeCH_2NH_3^+$	838
$H(N4)TrNMeCH_2NH_2^+$	802
$TrNMeHCH_2NH_2^+$	874
$TrNMeCH_2NH_2Me^+$	853
$H(N4)TrNMeCH_2NHMe^+$	805
$TrNMeHCH_2NHMe^+$	874
$TrNMeCH_2NHMe_2^+$	899
$H(N4)TrNMeCH_2NMe_2^+$	827
$TrNMeHCH_2NMe_2^+$	905
$TrNMeCH_2SH_2^+$	932
$H(N4)TrNMeCH_2SH^+$	837
$TrNMeHCH_2SH^+$	909
H_3O^+	567
CH_2OH^+	651
H_3NMe^+	677
$MeO(H)CH_2OH^+$	362
$H_2C{=}NH_2^+$	781
$H_2C{=}NHMe^+$	763
$H_2C{=}NMe_2^+$	762

N(9)–CH_2 and C(5)–N(9) bonds with corresponding decreases in bond order and a slight shortening of the C–X bond with increase in bond order; the N(9)-protonated HMPMM structure, for example, thus resembles PMM associated with protonated formaldehyde. Protonation of N-4 is always more favourable and is accompanied by stretching of the ring C–N(4) bonds to about 1.406 Å with only minor changes (±0.02 Å) in the side-chain bond lengths. The minimum enthalpy conformation has the lone pair of the electronegative atom in CH_2X directed towards the additional proton but these atoms are still fairly distant, their separation varying from 2.5 for X = NH_2 to 3.2 Å for X = NMe_2.

The structure of the iminium ion ($TrNMeCH_2^+$) produced by loss of water from *O*-protonated HMPMM was surprising at first. Although the nitrogen in the $CH_3NCH_2^+$ portion is

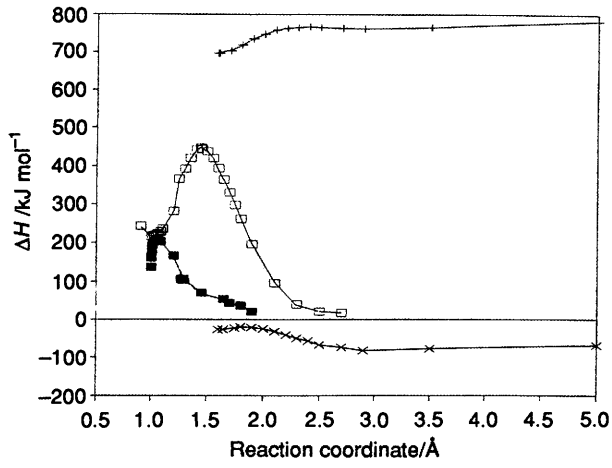

Fig. 2 MNDO calculated reaction pathways for the decomposition of HMPMM (**2**; $TrMeNCH_2OH$), its anion ($TrMeNCH_2O^-$) and protonated form ($TrMeNHCH_2OH^+$) by the mechanisms in Schemes 2, 3 and 4: (+) N-protonated, reaction coordinate = C(15)–N bond length; (□) concerted, reaction coordinate = N(4)–HO distance; (■) concerted IRC; (×) anionic, reaction coordinate = C(15)–N bond length

planar, with each bond angle to nitrogen being near 120°, this group is at 80° to the triazine ring. The bond order of the N–CH_2^+ is 1.73 instead of the usual N–CH_3 bond order of 0.86, while that of N(9)–C(5) is reduced from the usual 1.11 (in HMPMM for example) to 0.87. Thus formation of the iminium ion in which the positive charge is delocalized by partial double-bond formation to N removes the usual stabilization of the electron deficient triazine ring by conjugation with the same N. On the other hand, near orthogonality of the side group to the ring minimizes delocalization of the positive charge over the already electron-deficient ring.

Decomposition Reactions.—Location of the transition state of the concerted decomposition (Scheme 4) of HMPMM to give formaldehyde and a tautomer of PMM was not possible by gradual stretching of N–CH_2OH or of O–H. Starting at the ground state of HMPMM and gradually reducing the OH • • • N(4) distance gave a smooth change in enthalpy (Fig. 2), peaking at 448 kJ mol^{-1} when OH • • • N was 1.44 Å, but the structure at the peak did not have force constants characteristic of a transition state. Using a saddle calculation between structures on either side of this peak located an alternative structure, which could be optimized using eigenvector-following to an acceptable transition state structure at 212 kJ mol^{-1}. The true reaction path, labelled IRC in Fig. 2, was obtained by following the intrinsic reaction coordinate in both directions from the transition state. The very steep drop in enthalpy as the N • • • H distance is closed from the transition is similar to that previously found[1] for the concerted decomposition of hydroxymethyltriazenes and is accompanied by a significant increase in the N(9)–C(15) distance. The concerted reaction thus has an enthalpy change of 157 kJ mol^{-1} (for production of isolated molecules) and requires an activation energy of 290 kJ mol^{-1}. This is thus expected to be unfavourable at body temperature.

Loss of protonated formaldehyde from *N*-protonated HMPMM has a similar enthalpy change to the concerted decomposition but a smaller activation energy (126 kJ mol^{-1}). In this case (and most others examined) the reaction path (Fig. 2) obtained by partial optimization while stretching the reacting bond did give a structure at the peak close to that of the fully optimized transition state (Table 3).

The transition state for loss of formaldehyde from the anion

Table 3 MNDO calculated enthalpies of formation ($\Delta_f H$) for optimized transition-state geometries fully characterized by having a single negative force constant and six zero force constants. ΔH is the enthalpy difference between reactants and products, E_{act} is the activation energy, $\Delta_{taut}H$ is the enthalpy change when tautomerism places the proton on N-4 of the triazine

Reaction	Enthalpies/kJ mol^{-1}				Separation from C(15)/Å		
	$\Delta_f H$	ΔH	E_{act}	$\Delta_{taut}H$	O(33)	N(9)	Nu
$TrNMeCH_2O^- \longrightarrow TrNMe^- + CH_2O$	−42	−141	3	—	1.24	1.87	—
$TrNMeCH_2OH_2^+ \longrightarrow TrNMeCH_2^+ + H_2O$	721	−23	21	—	1.87	1.36	—
$TrNMeHCH_2OH^+ \longrightarrow TrNMeH + CH_2OH^+$	750	126	79	−158	1.29	2.35	—
$TrNMeCH_2OH \longrightarrow H(N4)TrNMe + CH_2O$	212	115	248	—	1.29	1.61	—
$TrNMeCH_2OH_2^+ + NH_3 \longrightarrow TrNMeCH_2NH_3^+ + H_2O$	677	−90	4	−36	1.86	1.36	3.19
$TrNMeCH_2^+ + NH_3 \longrightarrow TrNMeCH_2NH_3^+$	900	−67	−5	−36	1.34 (N33)	2.18	—
$TrNMeCH_2^+ + H_2S \longrightarrow TrNMeCH_2SH_2^+$	951	−16	3	−95	1.34 (S33)	2.18	—
$TrNMeCH_2^+ + H_2O \longrightarrow TrNMeCH_2OH_2^+$	721	23	44	−111	1.36	1.87	—
$TrNMeCH_2^+ + H_2NMe \longrightarrow TrNMeCH_2NH_2Me^+$	907	−47	7	−48	1.34 (N33)	2.08	—
$TrNMeCH_2^+ + NHMe_2 \longrightarrow TrNMeCH_2NHMe_2^+$	925	−5	21	−72	1.35 (N33)	2.08	—
$TrNMeCH_2^+ + MeOH \longrightarrow TrNMeCH_2O(Me)H^+$	746	38	54	−115	1.36	1.83	—
$TrNMeHCH_2OH^+ + MeOH \longrightarrow TrNMeH + MeO(H)CH_2OH^+$	507	77	76	−152	1.30	3.49	1.94
$TrNMeHCH_2NH_2^+ \longrightarrow TrNMeH + CH_2NH_2^+$	919	53	45	−74	—	2.11	—
$TrNMeHCH_2NHMe^+ \longrightarrow TrNMeH + CH_2NHMe^+$	908	35	34	−69	—	2.08	—
$TrNMeHCH_2NMe_2^+ \longrightarrow TrNMeH + CH_2NMe_2^+$	926	−18	21	—	—	2.50	—

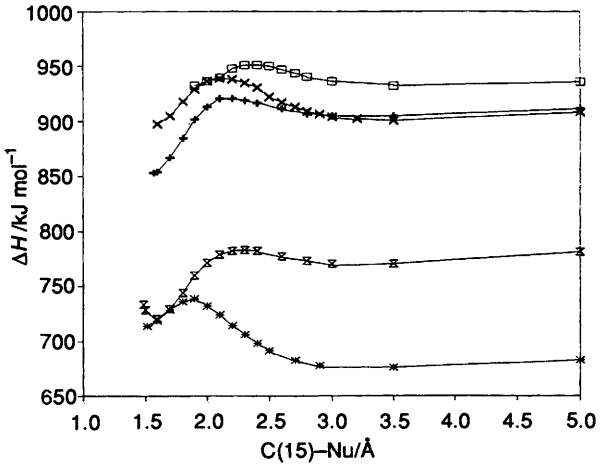

Fig. 3 MNDO calculated enthalpies of formation for optimized geometries on S_N1 reaction pathways (gradual reduction of $CH_2 \cdots Nu$ distance) for nucleophilic attack on *O*-protonated HMPMM (**2**): (□) $TrMeN{=}CH_2^+ + SH_2$, full optimization; (×) $TrMeN{=}CH_2^+ + NHMe_2$; (+) $TrMeN{=}CH_2^+ + NH_3$; (⊠) $TrMeN{=}CH_2^+ + MeOH$; (+) $TrMeNCH_2OH_2^+ \longrightarrow TrMeN{=}CH_2^+ + H_2O$

of HMPPM to give the anion of PMM was readily located by stretching the C(15)–N bond (Fig. 2). The reaction evolves 141 kJ mol^{-1} and full optimization of the transition state (Table 3) indicates an activation barrier of only 3 kJ mol^{-1} which means this is the most favoured decomposition route for basic or neutral conditions.

Nucleophilic Substitution Reactions.—S_N1 displacement reactions (Scheme 5 and Fig. 3) of HMPMM require initial loss of water from *O*-protonated HMPMM. This reaction proceeds exothermically ($\Delta H = -23$ kJ mol^{-1}) with only a small activation barrier (21 kJ mol^{-1}) to give the iminium ion. Reactions of this iminium ion with our model neutral nucleophiles were either exothermic or slightly endothermic (for MeOH and H_2O) and proceeded with small activation energies (20 to 76 kJ mol^{-1} when measured from the minimum energy of iminium ion associated with nucleophile, or −5 to 54 kJ mol^{-1} measured, as for E_{act} in Table 3, from the energy of fully optimized isolated reactants). In the case of SH_2 attachment of the sulfur took place without discernible activation energy when studied under partial optimization but when the reaction path was studied using full optimization and with steps of 0.05 Å in the C–S distance the position of the transition state was apparent and was easily optimized. Comparison of the activation energies involved gives the expected sequence of reactivity under kinetically controlled conditions to be $NH_3 > H_2S > H_2NMe > HNMe_2 > H_2O > MeOH$. Energy liberated during the reaction follows the same order except that $H_2NMe > H_2S$. The positively charged products ($TrNMeCH_2XH^+$), unlike the iminium ion, may tautomerize (the enthalpy changes are given under $\Delta_{taut}H$ in Table 3) making them more stable than [iminium ion + XH] even for the oxygen nucleophiles. Taking this into account one finds a thermodynamic preference for the reaction

$$TrNMeCH_2^+ + HX \longrightarrow H(N4)TrNMeCH_2X^+$$

to follow the order $H_2S > NH_3 > H_2NMe > H_2O > MeOH \approx HNMe_2$ for HX with overall enthalpies of reaction being −111, −103, −95, −88, −77 and −77 kJ mol^{-1} respectively. The position of the dimethylamine derivative at the end of the list is due to poor stabilization of the N(4)-protonated ion, because a steric clash between a methyl group and the triazine ring prevents adoption of the conformation preferred by the other $H(N\text{-}4)TrNMeCH_2X^+$. The activation energy for the reverse reactions, decomposition of $TrNMeCH_2XH^+$, is given by ($E_{act} - \Delta H$) and indicates the following order of X for kinetically-controlled reaction:

$$OMe > SH > OH > NMe_2 > NHMe > NH_2$$

These results suggest that HMPMM is likely to become linked to nitrogen and sulfur nucleophiles *in vivo*, but since the reactions have low activation energies for both forward and reverse reactions they will be reversible under physiological conditions. Whether such reversible alkylation of biomolecules would cause cytotoxicity is questionable but might explain the difference in biological effects from other alkylating agents which are irreversible. On the other hand a change to a more basic or less hydrophilic environment would render the protonated forms inaccessible and effectively make the reactions irreversible. In practise few reactions of hydroxymethylmelamines with nucleophiles have been reported but the methylene bis-(pentamethylmelamine), $TrNMeCH_2NMeTr$, is often found as a decomposition product of HMPMM—presumably decomposition gives PMM and the iminium ion which react to give the product; similar reactions result in the formation of polymeric resins from melamine and formal-

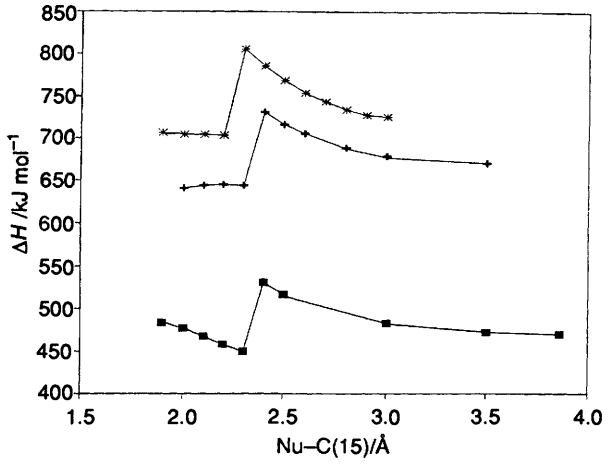

Fig. 4 MNDO calculated enthalpies of formation on the S_N2 reaction pathways (gradual reduction of $NCH_2 \cdots XH$ distance) for the reaction $TrNMeCH_2OH_2^+ + XH \longrightarrow TrNMeCH_2XH^+ + H_2O$: (■) MeOH; (+) NH_3; (✱) SH_2

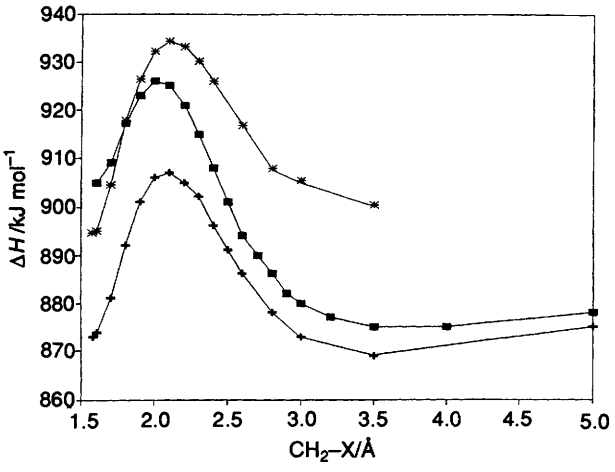

Fig. 5 MNDO calculated enthalpies of formation for the optimized geometries on the reaction pathways $TrN^+HMeCH_2NR^1R^2 \longrightarrow TrNHMe + {}^+CH_2NR^1R^2$ in which the $N\text{–}CH_2NR^1R^2$ bond is gradually stretched: X = NH_2 (✱); NHMe (+); NMe_2 (■)

dehyde. This makes our finding, that $H(N4)TrNMeCH_2NMe_2^+$ is the least thermodynamically stable $H(N4)TrNMeCH_2X^+$, surprising since steric hindrance to effective stabilization of the N(4)-protonated ion by the side-chain nitrogen N(33) is likely to be greater in the known bis compound ($TrNMeCH_2NMeTr$) than in the dimethylamino derivative. However, examination of framework molecular models suggests that excellent stabilization of the N(4)-protonated bis compound may be available if the extra proton is located between the two triazine rings. The large size of this ion means that calculations on its favoured conformation would be expensive and we have not attempted them.

From the point of view of drug design protonated HMPMM is one of the most reactive of the $TrNMeCH_2X$ molecules towards nucleophilic displacements—which are likely to be necessary for anticancer activity. However formation of the iminium ion $TrNMeCH_2^+$ from the protonated ethers, $TrNMeCH_2O(R)H^+$ is even less endothermic and requires less activation energy than protonated HMPMM, at least for R = Me, and so ethers are a worthwhile target for drug testing. An additional advantage is that the product from N(9)–C(15) cleavage of N(9)-protonated ethers is CH_2OR^+ which cannot immediately stabilize itself by loss of a proton. This unwanted decomposition is therefore less likely than for HMPMM itself.

The S_N2 displacements of H_2O from HMPMM protonated an oxygen by neutral molecules have negative or slightly positive enthalpy changes but were difficult to model partly due to the complex energy profile [17] of such reactions. The reaction profiles for reaction with SH_2, NH_3 and MeOH shown in Fig. 4 are the lowest of several found (differing in the conformation used to start the path calculation) and are typical in that approach of the nucleophile causes a gradual rise in energy until, while the attacking nucleophile is still quite distant, the water suddenly departs and the energy plummets. Extensive searches for transition states located one for attack by ammonia having $C \cdots NH_3 = 3.19$ and $C \cdots OH_2 = 1.86$ Å at 162 kJ mol^{-1} but we were unable to follow the intrinsic reaction coordinate to the aminal plus water and believe this is a minor transition between different complexes rather than a true transition state for the reaction. Our overall conclusion was that these reactions were disposed to be S_N1. Since our calculations relate to gas phase reactions they naturally favour S_N2 displacements and thus the calculated preference for S_N1 reactions is reinforced for aqueous conditions and S_N1 should then be expected virtually exclusively.

S_N2 reactions of HMPMM with nucleophiles such as SH^- or OMe^-, to liberate OH^-, were also very difficult to model, due to reasons given above and because of alternative removal of a proton from the carbon in CH_2OH, which occurred with nucleophiles, such as OMe^-, which were also strong bases. Reaction paths were similar in shape to those in Fig. 4 and although no transition state was unequivocally identified (by having a single negative force constant) indications were that the S_N2 reactions with MeO^-, OH^- or SH^- are unfavourable being endothermic and having higher activation energies (E_{act} = 120–300 kJ mol^{-1}) than the equivalent S_N1 reactions. Calculations on S_N2 reactions of HMPMM with neutral nucleophiles displacing OH^- were not run since there would be a large, difficult to calculate, change in solvation energy during such reactions. Also there is no reason to believe that these reactions would be any more favoured than the S_N2 reactions already discounted.

The S_N2 displacements of PMM from HMPMM protonated on N-9 gave similar reaction profiles to the displacements of H_2O. Again approach of the nucleophile often caused sudden departure of the leaving group (PMM) and S_N1 reactions are probably preferred even for the gas phase. The only transition state characterized was for attack by methanol but once again this was not a transition state for the complete reaction, just an interconversion of complexes.

For N(9)-protonated HMPMM, the S_N1 reaction is hampered by the relatively high enthalpy of protonated formaldehyde which departs. For N(9)-protonated aminals, $TrNHMeCH_2NR_2^+$, the leaving group is $CH_2NR_2^+$ which is much better stabilized by the nitrogen than protonated formaldehyde is by oxygen. We therefore examined the S_N1 decompositions of the protonated aminals and found the reaction pathways shown in Fig. 5. As shown in this figure and Table 3 the activation energies are quite low. For X = NMe_2 in $TrNMeCH_2X^+$ the decomposition is exothermic and the reaction is also exothermic for X = NH_2 and X = NHMe if subsequent transfer of a proton from the iminium ion to N(4) of PMM is included. Methylene iminium ions ($CH_2{=}X^+$) produced in these decomposition reactions readily react with active hydrogen compounds including ketones, alcohols and thiols (Mannich reaction) with the possible overall effect of linking biomolecules through CH_2 groups.

The picture that emerges for reactions of HMPMM with amines is a complex one. The ground state energies for molecules involved in the various reactions of a mixture of protonated HMPMM with H_2NMe are shown in Fig. 6. Most of the activation energies are reasonably low and so one expects

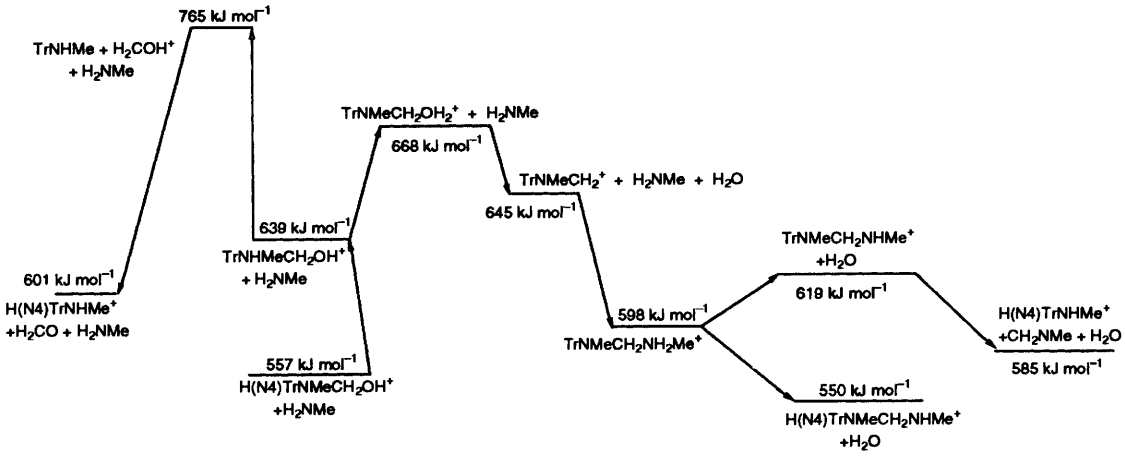

Fig. 6 MNDO calculated enthalpies of formation for the optimized ground-state geometries involved in reactions of protonated HMPMM (**2**) with H_2NMe

a build up of those compounds with lowest ground state energies. These findings are in accord with studies[18,9] showing that self-condensation reactions of melamine resins are reversible.

Conclusion

Our calculations predict that the reactions of HMPMM under physiological conditions are likely to be critically dependent on the pH. In neutral or basic solution deprotonation is feasible and is likely to be followed by rapid decomposition to formaldehyde and PMM. Under acidic conditions protonation on oxygen seems reasonable and may be followed by nucleophilic displacement by (in order of preference) N, S or O nucleophiles by S_N1 processes. Liberation of methylene iminium ions from the N(9)-protonated aminal products appears facile and their reaction with biomolecules might be important in the mechanism of antitumour action. The eigenvector following method for locating transition states has been found very effective at finding enthalpy maxima, even where the initially supplied geometry is poor, but may home in on a local enthalpy maximum even when a geometry close to the transition state for the overall reaction is supplied.

Experimental

Calculation Methods.—All calculations were run on a DEC 5830 computer at the University of Wales, Aberystwyth initially using the semiempirical MNDO method within the MOPAC program package[13] Version 2 (having the minimum modifications to run on the DEC 5830). First HMPMM was fully optimized and a global ground state sought by rotating all principal exocyclic bonds. The geometry of the 4,6-bis-(dimethylamino)-1,3,5-triazinyl moiety (Tr) was normally kept constant for optimization of the ground states of other molecules with optimization being limited to the variable side-chain and the ring carbon atom at the point of attachment. The values used were as in Fig. 1. These structures were then fully optimized using the default settings in MOPAC 93 except that optimization criteria were made 100 times more stringent by use of the keyword PRECISE. An exception to this general method was optimization of the trimelamols (**5**) which used full optimization in MOPAC 93 with the restriction that C_3 symmetry was maintained.

Energy profiles for reaction paths were obtained with constant bis-(dimethylamino)triazinyl moiety as above and with chemically equivalent atoms set with equal bond lengths and angles and symmetric dihedral angles. The profiles were obtained by increasing a bond broken in the reaction under study in 0.1 Å steps or by decreasing a bond length made during reaction. Once a smooth interconversion between starting materials and products was found this was selected for further study. Where smooth interconversions were not readily found for the forward reactions, reverse reactions were similarly examined. The S_N2 pathways were initially set-up to have the attacking nucleophile directly opposite N-9 (Nuc–C–N = 180°) but this angle of approach was then allowed to optimize as the nucleophile was placed closer. Since the triazinyl ring was not optimized and symmetry constraints were maintained the energies of the reaction profiles are higher than shown for the fully optimized stationary states.

The normal method for initial location of transition states was to use a saddle calculation between structures symmetrically situated on either side of the peak in the energy profile with symmetry and other constraints still applied. The best estimate of the transition state so obtained was then fully optimized without symmetry or other constraints using eigenvector following (the TS option[14] in MOPAC 93). For reaction profiles with broad peaks the saddle calculation could be omitted—direct optimization of the structure nearest the top of the reaction profile by eigenvector following was usually reliable and quicker. Finally the presence of a single negative force constant was confirmed (using a FORCE calculation) to characterize the structure as a true transition state.

References

1 Part 4: R. J. Simmonds, W. Mallawaarachchi, P. A. Mallawaarachchi and D. E. Parry, *J. Chem. Soc., Perkin Trans. 2*, 1993, 1399.
2 B. J. Foster, B. J. Harding, B. Leyland-Jones and D. Hoth, *Cancer Treat. Rev.*, 1986, 197.
3 C. J. Rutty and T. A. Connors, *Biochem. Pharmacol.*, 1977, **26**, 2385.
4 I. R. Judson, in *Triazenes. Chemical, Biological and Clinical Aspects*, ed. T. Giraldi, T. A. Connors and G. Cartei, Plenum Press, New York and London, 1990, 173.
5 M. M. Ames, M. E. Saunders and W. S. Tiede, *Cancer Res.*, 1983, **43**, 500.
6 S. J. Addison, B. D. M. Cunningham, E. N. Gate, P. Z. Shah and M. D. Threadgill, *J. Chem. Soc., Perkin Trans. 1*, 1985, 75.
7 M. Jarman, H. M. Coley, I. R. Judson, T. J. Thorton, D. E. V. Wilman, G. Abel and C. J. Rutty, *J. Med. Chem.*, 1993, **36**, 4195.
8 M. Johansen and H. Bundgaard, *Arch. Pharm. Chimi. Sci. Ed.*, 1979, **7**, 175.
9 T. Yoshii, T. Konakahara and K. Sato, *Makromol. Chem.*, 1987, **188**, 1683, and references therein.
10 H. E. Zaugg and W. B. Martin, *Organic Reactions*, 1965, **14**, 52.

11 W. Mallawaarachchi, G. M. Wright, R. J. Simmonds and D. E. Parry, *Anti-cancer Drug Design*, 1989, **4**, 233.
12 J. Iley, L. Fernandes and E. Rosa, *J. Chem. Soc., Perkin Trans. 2*, 1992, 223.
13 J. P. Stewart, MOPAC, QCPE Program No. 455, Quantum Chemistry Program Exchange, University of Indiana, Bloomington, Indiana, USA.
14 MOPAC 93, J. J. P. Stewart and Fujitsu, Tokyo, Japan; All Rights Reserved, Copyright Fujitsu Limited, 1993.
15 MOPAC 93 Manual, J. J. P. Stewart, Fujitsu Limited, Tokyo, Japan, 1993.
16 R. J. Simmonds, E. B. Katenga and C. Schwalbe, *Anti-cancer Drug Design*, 1988, **3**, 91.
17 T. Kozaki, K. Morihashi and O. Kikuchi, *J. Am. Chem. Soc.*, 1989, **111**, 1547.
18 U. Samaraweera and F. N. Jones, *J. Coatings Technol.*, 1992, **64**, 69.

Paper 4/05835F
Received 26*th September* 1994
Accepted 28*th November* 1994